

Shape coexistence in ^{68}Ni

S. Suchyta,^{1,2} S. N. Liddick,^{1,2} Y. Tsunoda,³ T. Otsuka,^{1,3,4,5} M. B. Bennett,^{1,4} A. Chemey,¹ M. Honma,⁶ N. Larson,^{1,2} C. J. Prokop,^{1,2} S. J. Quinn,^{1,4} N. Shimizu,⁵ A. Simon,¹ A. Spyrou,^{1,4} V. Tripathi,⁷ Y. Utsuno,⁸ and J. M. VonMoss⁷

¹National Superconducting Cyclotron Laboratory (NSCL), Michigan State University, East Lansing, Michigan 48824, USA

²Department of Chemistry, Michigan State University, East Lansing, Michigan 48824, USA

³Department of Physics, University of Tokyo, Hongo, Bunkyo-ku, Tokyo 113-0033, Japan

⁴Department of Physics, Michigan State University, East Lansing, Michigan 48824, USA

⁵Center for Nuclear Study, University of Tokyo, Hongo, Bunkyo-ku, Tokyo 113-0033, Japan

⁶Center for Mathematical Science, University of Aizu, Tsuruga, Ikki-machi, Aizu-Wakamatsu, Fukushima 965-8580, Japan

⁷Department of Physics, Florida State University, Tallahassee, Florida 32206, USA

⁸Advanced Science Research Center, Japan Atomic Energy Agency, Tokai, Ibaraki 319-1195, Japan

(Received 20 September 2013; revised manuscript received 4 November 2013; published 11 February 2014)

The internal-conversion and internal-pair-production decays of the first excited 0^+ state in ^{68}Ni are studied following the β decay of ^{68}Co . A novel experimental technique, in which the ions of ^{68}Co were implanted into a planar germanium double-sided strip detector and which required digital pulse processing, is developed. The values for the energy of the first excited 0^+ state and the electric monopole transition strength from the first excited 0^+ state to the ground state in ^{68}Ni are determined to be 1605(3) keV and $7.6(4) \times 10^{-3}$, respectively. Comparisons of the experimental results to Monte Carlo shell-model calculations suggest the coexistence between a spherical ground state and an oblate first excited 0^+ state in ^{68}Ni .

DOI: 10.1103/PhysRevC.89.021301

PACS number(s): 21.10.-k, 21.60.Cs, 23.35.+g, 27.50.+e

The development of shell structure is observed in a wide variety of interacting quantum systems including atoms [1], quantum dots [2], metal clusters [3], and atomic nuclei [4] and is characterized by sets of nearly degenerate energy levels separated by large-energy gaps due to an irregular spacing of the energy states available to a single particle moving within a mean field. In a nucleus with an even number of protons and neutrons, completely filling the available states below a large-energy gap predominately results in a spherical nucleus. However, the nucleus is susceptible to adopting a deformed shape, either prolate (American-football-like) or oblate (pancake-like), following a certain redistribution of a few nucleons across the energy gap that results in multiple particles above the closed shell and an equivalent number of holes below the shell gap [5]. The energy of the multiple-particle-multiple-hole excitation relative to the spherical closed shell is a subtle balance between the energy cost for promoting the particles across the shell gap and the energy gained from nucleon-nucleon interactions [5]. If the gain in energy is comparable to the shell gap, multiple competing shapes can coexist, and examples of coexisting spherical and deformed shapes have been observed (e.g., ^{16}O [6] or ^{186}Pb [7]).

The neutron-rich region near $N = 40$ has received significant attention due to the rapid development of collectivity observed following the removal of protons from the $f_{7/2}$ orbital, which is attributed to an increase in deformation. Ground-state deformations of $\beta_2 \sim 0.3$ have been inferred for the isotonic $^{66}\text{Fe}_{40}$ and $^{64}\text{Cr}_{40}$ nuclei based on the measured low energies of their respective first excited 2^+ states and correspondingly high $B(E2; 2_1^+ \rightarrow 0_1^+)$ values [8–11]. In $^{67}\text{Co}_{40}$, just one proton removed from ^{68}Ni , an isomeric state has been identified. The isomer is attributed to the prolate-deformed $\pi[321]1/2^-$ intruder configuration resulting from the excitation of protons

across the $Z = 28$ shell gap and has an excitation energy of only 492 keV relative to the spherical $7/2^-$ ground state [12]. Additional nuclei in the region have been inferred to have both low-energy spherical and deformed states and include $^{65,66,68}_{27}\text{Co}_{39,40,41}$ and $^{64,66}_{25}\text{Mn}_{39,41}$ [13–15].

Multiple low-energy 0^+ excited states have been observed in ^{68}Ni and are likely due to excitations across $Z = 28$ and $N = 40$. The first excited 0^+ state [16] has been interpreted primarily as a neutron two-particle-two-hole excitation across $N = 40$ [17,18]. Based on the presence of a deformed minimum accompanying the global spherical minimum in the ^{68}Ni potential energy surface in Ref. [19], the possibility of a prolate-deformed first excited 0^+ state was suggested. However, recent calculations present a qualitatively different deformation for the first excited 0^+ state, predicting the state to be oblate [20]. The corresponding proton two-particle-two-hole 0^+ excited state in ^{68}Ni has not been conclusively identified. The 2511-keV 0^+ state [21,22] has been suggested as a possible candidate [17,18]. A third excited 0^+ state was claimed at 2202 keV in ^{68}Ni [23], but the state has not been observed in other experimental work [22].

Despite the numerous experimental and theoretical undertakings, a complete knowledge of the nuclear structure of ^{68}Ni has not been achieved. Although the first excited 0^+ state in ^{68}Ni was identified over 30 years ago [16], its energy is still not well known. In this Rapid Communication, we report on the precise determination of the energy and decay strength of the first excited 0^+ state in ^{68}Ni and extract a difference in deformation between the excited 0^+ state and the ground state consistent with state-of-the-art theoretical calculations.

The β decay of ^{68}Co was used to populate the first excited 0^+ state in ^{68}Ni [14]. Ions of ^{68}Co were produced through the fragmentation of a 130 MeV/nucleon ^{76}Ge beam on a ^9Be target at the Coupled Cyclotron Facility of the

National Superconducting Cyclotron Laboratory (NSCL) and isolated using the A1900 fragment separator [24]. The ^{68}Co ions implanted a few millimeters deep into a novel planar germanium double-sided strip detector (GeDSSD) [25], which recorded the position and arrival time of each ion and the subsequent β -decay electrons. The GeDSSD was surrounded by an ancillary photon array, SeGA [26], to detect β -delayed γ rays.

A new experimental technique was used to extract the information about the decay of the first excited 0^+ state in ^{68}Ni , which occurred rapidly [$t_{1/2} = 268(12)$ ns] following the ^{68}Co β decay. Photon emission from the first excited 0^+ state is prohibited and the state decays to the ground state via an internal transition, either internal conversion or internal pair production. The selective identification of the internal transition in the presence of the interfering β -decay electrons relied on the isomeric nature of the 0^+ state and required the implementation of the novel planar GeDSSD detection system combined with digital pulse-shape processing techniques. The experimental signature is the linear sum of two discrete signals in the detector, the β -decay electron followed by the internal-conversion decay or the electron-positron pair production. The time profile of the process, shown in Fig. 1(a), is unique to this decay mode and was only recoverable using modern digital-data acquisition. The energies of the β -decay electron and internal transitions were extracted by comparing the detector signal with an experimentally derived idealized pulse shape by varying the amplitude and time offset of the ideal pulse [27]. The ideal pulse shape was created by averaging about 500 pulses from the 662-keV γ ray of a ^{137}Cs source. It should be noted that the processing technique used is universally applicable to any time-domain signal consisting of a linear sum of two independent components offset from each other in time and could be generalized to the study of a wide class of isomeric states. The energy of the internal transitions was determined from the amplitude of the second rise of signals having the characteristic shape shown in Fig. 1(a).

The energy spectrum of all signals attributed to the detection of a single electron or γ ray in the GeDSSD within 2 s following the implantation of a ^{68}Co ion is shown as the upper (blue) curve in Fig. 1(b). The single peak at 491 keV results from random correlations between the implantation of a ^{68}Co ion and the γ -ray decay of ^{67m}Co [12], a beam contaminant independently produced, identified, and implanted into the GeDSSD. The small subset of events resulting from the detection of two sequential radiations in the GeDSSD were identified by the characteristic “stair-step” pulse shape shown in Fig. 1(a). The energy spectrum of the isomeric decays is shown as the lower (red) curve in Fig. 1(b). The half-life extracted from the time difference between the detection of the β -decay electron and the internal transition is 268(12) ns, in agreement with the half-life of the first excited 0^+ state in ^{68}Ni determined from previous experimental work [28]. The 1604-keV peak results from the simultaneous detection of the electron from the internal-conversion decay of the first excited 0^+ state in ^{68}Ni and the accompanying 8.3-keV x ray [29] originating from the filling of the atomic-electron vacancy. The 570-keV peak is due to the simultaneous detection of the electron and positron created by the internal pair-production

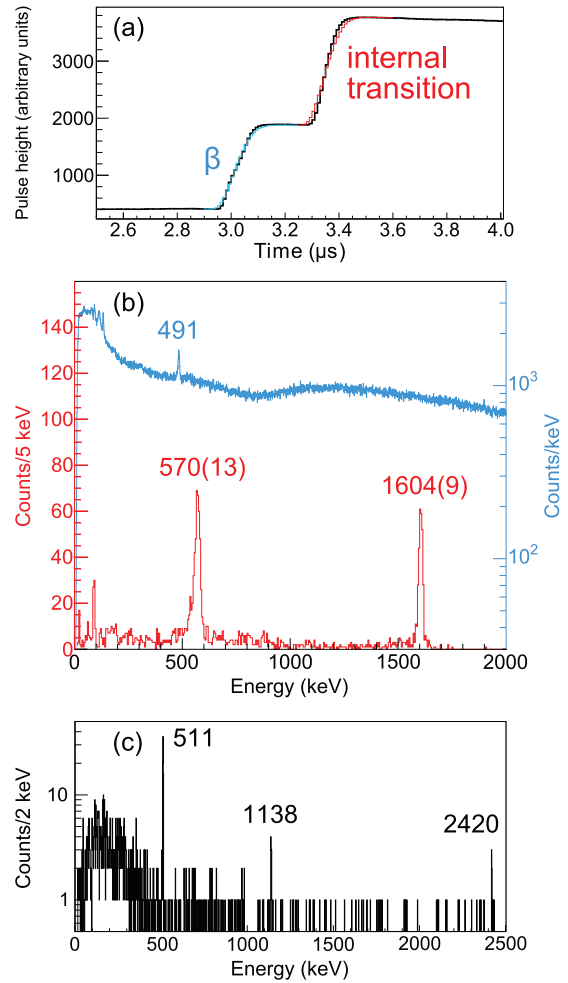


FIG. 1. (Color online) (a) Time profile of a GeDSSD detector signal for a ^{68}Co β decay followed by an internal transition. (b) Energy spectra measured in the GeDSSD for events which occurred less than 2 s following the arrival of a ^{68}Co ion, showing signals attributed to the detection of a single β -decay electron or γ ray (upper, blue curve) and signals due to the detection of sequential radiations within 600 ns of each other in the GeDSSD (lower, red curve). The peaks at 570 and 1604 keV are attributed to the detection of internal transitions from the first excited 0^+ state to the ground state in ^{68}Ni following β decay of ^{68}Co . (c) The γ -ray energy spectrum detected by SeGA in coincidence with “stair-step” signals in the GeDSSD.

decay of the first excited 0^+ state. The two 511-keV photons emitted following the positron annihilation typically escape the GeDSSD undetected. The energy difference of 1.034(16) MeV between the 1604- and 570-keV peaks matches the expected energy of 1.022 MeV necessary to create the electron-positron pair. No peaks near 1604 or 570 keV were detected in SeGA with sufficient intensity to suggest either are due to γ -ray transitions.

Three γ rays at 511, 1138, and 2420 keV were detected by SeGA in coincidence with the stair-step traces observed in the GeDSSD [see Fig. 1(c)]. The 511-keV peak results from the detection of the annihilation photons associated with the pair-production decay and is only coincident with the 570-keV

pair-production peak. The absolute intensity of the 511-keV γ rays in Fig. 1(c) is consistent with two 511-keV photons emitted for each count in the 570-keV peak. The 1138-keV transition, which was previously observed following the β decay of ^{68}Co but incorrectly placed feeding the isomeric 5^- state in ^{68}Ni [21], is instead assigned as depopulating the 2^+ state at 2743 keV [21,22] and feeding the first excited 0^+ state. The 2420-keV γ ray in Fig. 1(c) is observed for the first time and proposed to depopulate the 4026-keV state [21]. Possible feeding from other, higher-energy 2^+ states in ^{68}Ni are below experimental sensitivities. A transition between the first excited 2^+ and first excited 0^+ states was not observed and from the Monte Carlo shell-model calculations described below is calculated to be 0.5% of the intensity of the transition between the first excited 2^+ and ground state, which is below our experimental sensitivity. Based on the delayed photons of 1138 and 2420 keV and the known excitations of the levels they depopulate, the adopted energy of the first excited 0^+ state in ^{68}Ni is 1605(3) keV. The value of the electric monopole transition strength, $\rho^2(E0)$, for the transition between the first excited 0^+ state and ground state in ^{68}Ni is found to be $7.6(4) \times 10^{-3}$ using the energy of 1605(3) keV, a half-life of 268(12) ns, and the method of calculation described in Ref. [30].

The excitation energy and $\rho^2(E0)$ value of the first excited 0^+ state in $^{68}\text{Ni}_{40}$ can be compared to its proton analog, $^{90}\text{Zr}_{50}$. Two 0^+ states are also found below 2 MeV in ^{90}Zr and are associated with a pair of protons occupying either the $p_{1/2}$ or $g_{9/2}$ single-particle state. There is significant experimental evidence for strong mixing between the two 0^+ configurations, which results in the observed 0^+ ground state and 0^+ excited state at 1761 keV and the $\rho^2(E0)$ value of $3.46(14) \times 10^{-3}$ between the two states [31,32]. The $E0$ operator can be formulated as a sum over all nucleons of the effective charge of a given nucleon multiplied by the square of its position relative to the center of mass of the nucleus. Given equivalent nucleon excitations for ^{68}Ni and ^{90}Zr (two neutrons promoted across $N = 40$ or two protons promoted across $Z = 40$, respectively), the ratio of their respective $\rho^2(E0)$ values is proportional to the square of the ratio of the neutron and proton effective charges. Within the f_5pg_9 model space ($f_{5/2}$, $p_{3/2}$, $p_{1/2}$, and $g_{9/2}$ orbits), which has been used for both ^{68}Ni and ^{90}Zr , the square of the ratio of the neutron and proton effective charges can range from 0.25 to 0.54 [33–35]. Thus it might be expected that, if the predominant excitation in ^{90}Zr is of proton nature and that in ^{68}Ni is of neutron nature, the electric monopole transition strength in ^{68}Ni should be lower than in ^{90}Zr , but this is not observed experimentally. Motivated by the differences in 0^+ excitation energy and electric monopole transition strength between ^{68}Ni and ^{90}Zr , we performed shell-model calculations.

The ^{68}Ni nucleus is a key benchmark to understand how nuclei evolve as a progression is made from stability to increasingly exotic systems. Different theoretical interactions have been used in shell-model (SM) calculations for ^{68}Ni , and the calculated energy of the first excited 0^+ state ranges from 1.2 to 2.1 MeV (see Fig. 2). We have carried out systematic Monte Carlo shell-model (MCSM) calculations [20,37] with the A3DA effective interaction with minor revisions [20] on exotic Ni isotopes in a large configuration space comprising the full fp -shell orbits and the $g_{9/2}$ and

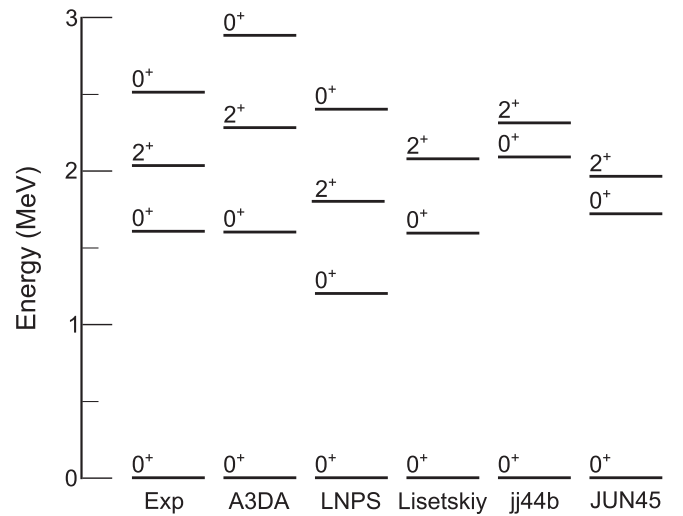


FIG. 2. Comparison of the experimentally determined energies of the three lowest-energy 0^+ states and the lowest-energy 2^+ state in ^{68}Ni (Exp) with theoretical calculations. Theoretical results are given for MCSM calculations using the revised A3DA interaction [20] and SM calculations using the LNPS [18], Lisetskiy [33], jj44b [34], and JUN45 [35] interactions. The experimental excitation energies of the second excited 0^+ state and the first excited 2^+ state were taken from Ref. [21] and Ref. [36], respectively.

$d_{5/2}$ single-particle states. Details regarding the MCSM results across the Ni isotopic chain will be provided in another publication [38]. Herein we focus on the results for ^{68}Ni , in particular for the first excited 0^+ state. The calculated energies of the 0_1^+ , 0_2^+ , 0_3^+ , and 2_1^+ states in ^{68}Ni from the present MCSM calculation, as well as the calculated energies of these states from SM calculations using several different effective interactions, are compared to experiment in Fig. 2. Only those states calculated to be below 3 MeV are shown in Fig. 2.

A key aspect of each calculation is the valence space used. The Lisetskiy, jj44b, and JUN45 calculations are performed in the f_5pg_9 model space, meaning that there are no valence protons for ^{68}Ni and proton excitations are not explicitly included. On the other hand, the MCSM and LNPS calculations explicitly include proton excitations in the valence space. The second excited 0^+ state in ^{68}Ni has been proposed to be due to proton excitations [17,18]. The prediction of three 0^+ states below 3 MeV by just the MCSM and LNPS calculations (and not by the Lisetskiy, jj44b, and JUN45 calculations) highlights the importance of the additional proton degrees of freedom. It should be noted the more restrictive model space that does not consider the full fp shell can reproduce the energy of the first excited 0^+ state (the calculation using the Lisetskiy interaction in Fig. 2, for example). However, it is likely due to the implicit incorporation of proton excitations in the effective interaction [33], and the predicted nucleon configuration of the first excited 0^+ state is different between the calculations in the different model spaces.

The low-energy level scheme of ^{68}Ni determined from the present MCSM calculation compares favorably to experiment, reproducing the energy of the first excited 0^+ state and

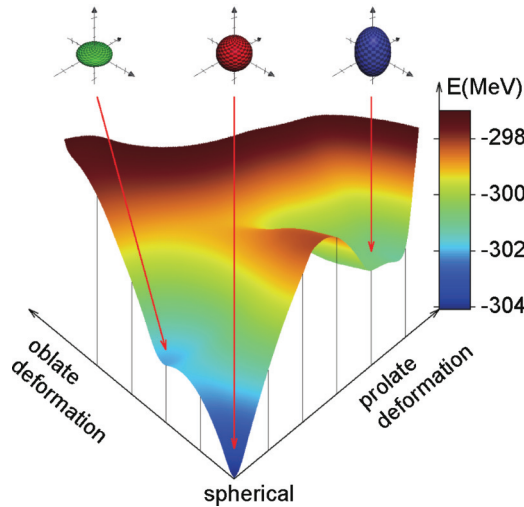


FIG. 3. (Color online) The energy of ^{68}Ni as a function of a given ellipsoidal shape. The energy was obtained by a Hartree-Fock calculation constrained by the quadrupole moment for the Hamiltonian being used. Each tick along the axis corresponds to an increment of $50 e\text{fm}^2$ in the magnitude of the quadrupole moment.

predicting three 0^+ states below 3 MeV. The potential energy surface for ^{68}Ni is shown in Fig. 3 and suggests that each 0^+ state is associated with a characteristic shape: spherical, oblate, or prolate. The calculated ^{68}Ni ground state has strong overlap with MCSM basis states with small quadrupole moments (and located near the deep spherical absolute minimum in Fig. 3), which indicates that the ground state of ^{68}Ni is spherical. In a similar manner, the local minima in the potential energy surface present at oblate and prolate deformations correspond to the first and second excited 0^+ states, respectively. The first excited 0^+ state has, on average, 0.7 protons and 2.4 neutrons excited across the conventional $Z = 28$ and $N = 40$ gaps, respectively. The MCSM results indicate that the first excited 0^+ and 2^+ states are members of the same rotational band and the 2^+ state has a quadrupole moment indicative of oblate shape.

The magnitude of the electric monopole transition strength from the first excited 0^+ state to the ground state in ^{68}Ni is a sensitive indicator of the underlying nucleon configuration. However, the value is very difficult to directly predict due to an incomplete knowledge of the appropriate effective charges. In order to extract information beyond the energy of the excited 0^+ state from the experimental measurement that can be

compared to current theories, the difference in mean-square charge radii between the ground and first excited 0^+ states in ^{68}Ni can be inferred from the measured $\rho^2(E0)$ value given a value for the mixing between the two underlying configurations using a simple two-level mixing model [31]. Based on measurements of relative $B(E2)$ values for the deexcitations of the 2_1^+ and 2_2^+ states, Recchia *et al.* [39] have inferred a large degree of mixing due to nucleon particle-hole excitations in ^{68}Ni . Additionally, large mixing amplitudes have also been inferred for the ground and first excited 0^+ states in ^{90}Zr , assumed to be the proton analog of ^{68}Ni , within a two-level mixing model [31,40]. By assuming maximal mixing between the spherical and oblate 0^+ configurations, a difference in mean-square charge radii of 0.15 fm^2 is determined. Under the assumption that this difference can be represented by an axial deformation, a difference in the absolute values of the intrinsic quadrupole moments of $102 e\text{fm}^2$ is obtained, which is consistent with the value of $-95 e\text{fm}^2$ predicted by the MCSM calculation (see Fig. 3).

In conclusion, the decay of the first excited 0^+ state in ^{68}Ni has been studied following the β decay of ^{68}Co . Using a novel planar germanium double-sided strip detector and a new experimental technique incorporating modern digital data acquisition and pulse processing, the precise energy and decay strength of the first excited 0^+ state in ^{68}Ni was determined. Monte Carlo shell-model calculations give a coherent description of the experimental results and suggest that spherical, oblate, and prolate shapes appear within the energy range of 3 MeV in ^{68}Ni . The combined experimental and theoretical results of the present study provide valuable insight on the nuclear structure of ^{68}Ni , a key nucleus to understand as a transition is made from stable to very neutron rich nuclei.

Note added in proof. The energy of the first excited 0^+ state in ^{68}Ni has also been independently verified in two-neutron-knockout and multinucleon-transfer reactions [39].

This work was funded in part by the NSF under Contracts No. PHY-1102511 (NSCL) and No. PHY-10-64819 (FSU), by the DOE under Contract No. DENA0000979 (NNSA), and by MEXT Grant-in-Aid for Scientific Research (A) 20244022. This work has been supported in part by HPCI (hp120284 and hp130024), and is a part of the RIKEN-CNS joint research project on large-scale nuclear-structure calculations. Y.T. acknowledges support by a JSPS for research grant (No. 258994).

- [1] N. Bohr, *Philos. Mag.* **26**, 1 (1913).
- [2] S. Tarucha, D. G. Austing, T. Honda, R. J. van der Hage, and L. P. Kouwenhoven, *Phys. Rev. Lett.* **77**, 3613 (1996).
- [3] W. D. Knight, K. Clemenger, W. A. de Heer, W. A. Saunders, M. Y. Chou, and M. L. Cohen, *Phys. Rev. Lett.* **52**, 2141 (1984).
- [4] M. G. Mayer and J. H. D. Jensen, *Elementary Theory of Nuclear Shell Structure* (Wiley, New York, 1955).
- [5] K. Heyde and J. L. Wood, *Rev. Mod. Phys.* **83**, 1467 (2011).
- [6] H. Morinaga, *Phys. Rev.* **101**, 254 (1956).
- [7] A. N. Andreyev *et al.*, *Nature (London)* **405**, 430 (2000).

- [8] M. Hannawald *et al.* (ISOLDE Collaboration), *Phys. Rev. Lett.* **82**, 1391 (1999).
- [9] W. Rother *et al.*, *Phys. Rev. Lett.* **106**, 022502 (2011).
- [10] A. Gade *et al.*, *Phys. Rev. C* **81**, 051304(R) (2010).
- [11] H. L. Crawford *et al.*, *Phys. Rev. Lett.* **110**, 242701 (2013).
- [12] D. Pauwels *et al.*, *Phys. Rev. C* **78**, 041307(R) (2008).
- [13] D. Pauwels *et al.*, *Phys. Rev. C* **79**, 044309 (2009).
- [14] S. N. Liddick *et al.*, *Phys. Rev. C* **85**, 014328 (2012).
- [15] S. N. Liddick *et al.*, *Phys. Rev. C* **84**, 061305 (2011).
- [16] M. Bernas, P. Dessagne, M. Langevin, J. Payet, F. Pougheon, and P. Roussel, *Phys. Lett. B* **113**, 279 (1982).

- [17] D. Pauwels, J. L. Wood, K. Heyde, M. Huyse, R. Julin, and P. Van Duppen, *Phys. Rev. C* **82**, 027304 (2010).
- [18] S. M. Lenzi, F. Nowacki, A. Poves, and K. Sieja, *Phys. Rev. C* **82**, 054301 (2010).
- [19] M. Girod, P. Dessagne, M. Bernas, M. Langevin, F. Pougheon, and P. Roussel, *Phys. Rev. C* **37**, 2600 (1988).
- [20] N. Shimizu, T. Abe, Y. Tsunoda, Y. Utsuno, T. Yoshida, T. Mizusaki, M. Honma, and T. Otsuka, *Prog. Theor. Exp. Phys.* **2012**, 1A205 (2012).
- [21] W. F. Mueller *et al.*, *Phys. Rev. C* **61**, 054308 (2000).
- [22] C. J. Chiara *et al.*, *Phys. Rev. C* **86**, 041304 (2012).
- [23] A. Dijon *et al.*, *Phys. Rev. C* **85**, 031301 (2012).
- [24] D. J. Morrissey, B. M. Sherrill, M. Steiner, A. Stolz, and I. Wiedenhoever, *Nucl. Instrum. Methods Phys. Res. B* **204**, 90 (2003).
- [25] N. Larson, *et al.*, *Nucl. Instrum. Methods Phys. Res. A* **727**, 59 (2013).
- [26] W. F. Mueller, J. A. Church, T. Glasmacher, D. Gutknecht, G. Hackman, P. G. Hansen, Z. Hu, K. L. Miller, and P. Quirin, *Nucl. Instrum. Methods Phys. Res. A* **466**, 492 (2001).
- [27] S. Liddick, I. Darby, and R. Grzywacz, *Nucl. Instrum. Methods Phys. Res. A* **669**, 70 (2012).
- [28] O. Sorlin *et al.*, *Phys. Rev. Lett.* **88**, 092501 (2002).
- [29] J. A. Bearden and A. F. Burr, *Rev. Mod. Phys.* **39**, 125 (1967).
- [30] T. Kibédi, T. Burrows, M. Trzhaskovskaya, P. Davidson, and C. N. Jr., *Nucl. Instrum. Methods Phys. Res. A* **589**, 202 (2008).
- [31] J. Wood, E. Zganjar, C. D. Coster, and K. Heyde, *Nucl. Phys.* **651**, 323 (1999).
- [32] T. Kibédi and R. Spear, *At. Data Nucl. Data Tables* **89**, 77 (2005).
- [33] A. F. Lisetskiy, B. A. Brown, M. Horoi, and H. Grawe, *Phys. Rev. C* **70**, 044314 (2004).
- [34] B. Cheal *et al.*, *Phys. Rev. Lett.* **104**, 252502 (2010).
- [35] M. Honma, T. Otsuka, T. Mizusaki, and M. Hjorth-Jensen, *Phys. Rev. C* **80**, 064323 (2009).
- [36] R. Broda *et al.*, *Phys. Rev. Lett.* **74**, 868 (1995).
- [37] T. Otsuka, M. Honma, T. Mizusaki, N. Shimizu, and Y. Utsuno, *Prog. Part. Nucl. Phys.* **47**, 319 (2001).
- [38] Y. Tsunoda, T. Otsuka, N. Shimizu, M. Honma, and Y. Utsuno (unpublished).
- [39] F. Recchia *et al.*, *Phys. Rev. C* **88**, 041302 (2013).
- [40] A. V. D. Berg, A. Saha, G. Jones, L. Put, and R. Siemssen, *Nucl. Phys. A* **429**, 1 (1984).